

FDTD based Plasmonic Light Trapping Analysis in Thin Film Hydrogenated Amorphous Silicon Solar Cells

Chetan Radder*, B S Satyanarayana**

* Electronics Engineering, Jain University, Bangalore, India

** BML Munjal University, Sidhrawali, Gurgaon, India

(chetanradder89@gmail.com, satyang10@gmail.com)

‡Chetan Radder, Electronics Engineering, Jain University, Bangalore,

Tel: +91 9481107705, chetanradder89@gmail.com

Received: 06.09.2017 Accepted:17.11.2017

Abstract- For thin film solar cells, plasmonics is a novel light trapping technique based on light scattering due to metal nanoparticles through excitation of localized surface plasmons. The excited surface plasmon at the interface of a higher dielectric active semiconducting layer and the metal, by channelling incident radiations will trap light within the device for the higher optical path in physically thin structures resulting in enhanced photocurrent. In this paper, through FDTD based electromagnetic simulations, significance of controlled nanopatterning of silver (Ag) on the front side of p-i-n hydrogenated amorphous silicon for light absorption in the devices is analyzed. The analysis includes better control of nanoparticle parameters like size, shape, distribution and spacing for obtaining full benefits of plasmonic effects. It is demonstrated with an attractive strategy of fine tuning the nanostructures, incident light coupling with semiconductor ensures light confinement within the active layer promoting photon absorption across visible and near infrared regions.

Keywords Photovoltaics; Thin Film Solar cells; Hydrogenated amorphous silicon solar cells; Silver nanoparticles; Surface Plasmons; Light trapping.

1. Introduction

In today's technology driven generation, eco-friendly renewable sources of energy need to match to that of fossil fuels with the expectation of cross over in the coming years as the source of energy generation [1,2]. For harvesting freely available solar radiations and to match to that of fossil fuels efficiency, available solar cells need to absorb all the incident light radiations induced with advanced techniques for energy conversion [3]. For any system to be successful and sustainable for a long duration, it has to be economically viable and highly efficient [4]. The material and fabrication cost is less in hydrogenated amorphous silicon (a-Si:H) solar cells with thin physical layers and with the reduced optical layers, light absorption also drastically reduces [5]. For efficient light-harvesting in thin film solar cells, the technique of plasmonics is illustrated which makes it possible to obtain optically thick for complete light absorption and physically thin for less material consumption and efficient carrier transportation in photosensitive layers [6].

In a silicon solar cell with a typical bandgap of $\sim 1.8\text{eV}$, over 50% of the transmitted solar radiation is unutilized by the cell. More focus is on the light management schemes for total utilization of above-bandgap photons in silicon solar devices. The silicon cannot absorb red light due to its material property and the introduction of metal nanoparticles (MNPs) on the front surface of a device will help the structure in absorbing red light of the visible spectrum [7]. The MNPs on the front side of thin film a-Si:H undergoes the localized surface plasmon resonance (LSPR) upon interaction with incident radiations, producing an enhanced localized optical field intensity surrounding nanoparticle resulting in the incident light being scattered in a wide range of angles increasing the optical path length in absorber layer [8]. Once incident light interacts with MNPs electromagnetic field invokes between MNPs and semiconductor layer giving rise to an optical transition rate proportional to the square of electric field amplitude resulting in increased photo-generation of electron-hole pairs, consequently increasing photocurrent in the device. At a particular resonating frequency, scattering size of the nanoparticle is more than

that of its physical size which leads to the formation of surface plasmon polariton (SPP) wave oscillation across metal/dielectric interface and at this metal property dependent frequency light scattering within the high dielectric absorbing layer will be maximum. SPP waves exist at the interface between materials only if the real part of the permittivity undergoes a sign change at the interface. Due to their abundance of free electrons, metals provide a negative real permittivity that ensures a sign change in permittivity at a metal/dielectric interface. The two main phenomena which take place between MNP and optical layers are light scattering and near-field concentration of light, the nanoparticle size and shape with the electrical design and its semiconductor absorption decides the precedence of one over the other in solar cells.

The main objective of the work is to develop the pattern for MNP placements for the maximum possible incident light absorption within the thin film device. The developed structural model solves Maxwell's equation to obtain the electric field displacement in the device upon interaction with the incident radiations calculating the near-field concentration of the MNPs and Mie scattering principle is applied to obtain the extinction cross sections and corresponding efficiencies based on the dielectric values of the medium with the generated field at the interface.

$$\frac{\partial D}{\partial t} = \nabla * H - J \quad (1)$$

where H is the magnetic field, D is the electric field displacement, J is the electric charge current density. Eq.(1) is the Maxwell's equation for generating time dependent electric field displacement.

$$\alpha = 4\pi a^3 \left(\frac{\frac{\epsilon_p}{\epsilon_m} - 1}{\frac{\epsilon_p}{\epsilon_m} + 2} \right) \quad (2)$$

Upon incident light radiations of wavelength λ with the MNP of radius a , polarizability α will be in resonance state when $\epsilon_p = -2\epsilon_m$ as mentioned in Eq.(2). The scattering (C_{sca}) and absorption (C_{abs}) cross sections are calculated from Eq.(3) and Eq.(4) based on Mie scattering principle.

$$c_{sca} = \frac{1}{6\pi} \left(\frac{2\pi}{\lambda} \right)^4 \alpha^2 \quad (3)$$

$$c_{abs} = \left(\frac{2\pi}{\lambda} \right) \text{Im}|\alpha| \quad (4)$$

In this paper, on the developed model based on the above equations, an analysis is done considering the structure with silver (Ag) nanoparticles on the front surface of a-Si:H solar cell to understand the plasmonic induced scattering and electric field effects on light absorption enhancement in the solar cell. Simulations were performed with three dimensional finite difference time domain (FDTD) approach for solving Maxwell equations to determine E-field

distribution and using Mie-scattering principle extinction efficiencies were calculated.

2. Structure Design and Simulation

A typical single junction p-i-n superstrate a-Si:H solar cell is considered on which MNPs are deposited, for the systematic study of the role of nanoparticle sizes, shapes, periodicity and coverage area on the light absorption in active photovoltaic layers of the solar structure. Fig.1 provides the schematic of single junction a-Si:H cell with nanoparticles on the front surface, along with the excitation scheme and the field monitors used in our FDTD simulations. The periodic metal nanostructures are stretched in x-z plane with the structure extending along y axis and perfectly matched layer (PML) boundary conditions across all the planes. The thickness of p, i and n layers were set to 10, 460 and 30nm respectively. The spacing between excitation incident surface and silver nanoparticles is constantly maintained at 200nm. Field monitors placed close to the particle for absorption measurement and outside the particle beyond the source to measure device scattering, named as right, left, top and bottom with unseen front and back as shown in Fig.1 covering all sides of the structure.

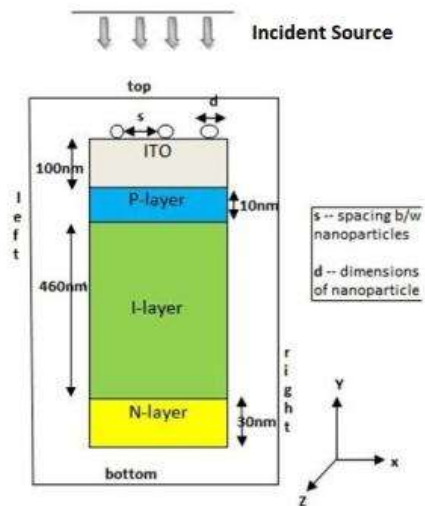


Fig. 1. Simulation model for MNP enabled single junction a-Si:H solar cell.

The FDTD approach covering responses for a range of frequencies is the most widely used time domain discretization method for numerical simulations of plasmonic structures with arbitrary and complex structures for calculation of electromagnetic fields in a single run of simulation. The three-dimensional MEEP simulator [9] is used for design and modelling of nanoparticle integrated thin film solar cells. The MEEP compatible FDTD code in scheme language was developed to calculate localized electromagnetic fields by solving Maxwell's equation. The generalized code constituting of device structure, material properties, incident source, nanostructures and monitors for flux calculation is used for various simulations with altering shapes, sizes, periodicity and area coverage for complete plasmonic analysis on single junction a-Si:H solar cell.

In plasmonic structures, out of the two incident polarizations: Transverse Magnetic(TM) (H-field along the metal strips) and Transverse Electric (TE) (E-field along the metal strips), SPP and LSPR are seen only with TM polarizations. So to explore plasmonic resonance across the interface incident TM polarized Gaussian wave (H_z) tuned between 350 nm and 750 nm is used in all the calculations. The optical properties of materials are defined by its dielectric value and in our analysis wavelength dependent dielectric values are used for optical simulations. The material dielectric values of ITO/Ag are picked from Ref [10] and that of p, i, n layers from Ref [11] and are converted to Lorentz Drude values for defining materials in FDTD simulations. The layers of thin film a-Si:H are electrically modelled with ohmic contacts between MNP and layers.

In our simulations, only the spectrum range from 200 to 700 nm is considered, as it is the range where a-Si:H absorption is concentrated. Mie theory simulations, although only valid for spherical particles with the diameter less than or equal to the wavelength of incident radiations, are often used to get a rough indication of the behaviour of plasmonic nanoparticles of various shapes. As the light of wavelength λ interacts with small (diameter $d \ll \lambda$) metallic particles, extinction behaviour due to resonant excitation of electron oscillations in the metal is observed. The extinction behaviour is the combination of scattering and absorption cross sections dependent on size, shape variations of nanoparticles.

The complex dielectric function of MNP consists of real and imaginary part values where the real part of the permittivity describes how strongly a material is polarized by an external electric field and the imaginary part describes the losses in the material due to the polarization and ohmic losses [12]. For visible and near infrared light the real part of the dielectric function of silver becomes more negative with increasing wavelength. This implies that when a silver particle is embedded in a non-absorbing medium, which by definition has a positive dielectric function, at a certain wavelength $\epsilon_p \approx -2\epsilon_m$ (ϵ_p is NP and ϵ_m is medium dielectric function), the polarizability will reach a maximum. At this so-called resonance wavelength, the polarizability is very large and the absorption and scattering cross-sections can exceed the geometrical cross-section by an order of magnitude.

3. Results and Discussions

The photocurrent enhancement due to improved forward scattering and tuning of surface plasmon resonance along the near infrared region depends on particle size, shape, mutual arrangement, concentration, and local dielectric environment apart from metals permittivity function [5,13].The complex geometry and position of nanoparticle (NP) can sometime suppress photocurrent by blocking incident light radiations. For wavelengths below 400nm, a-Si:H is highly absorbing and with increasing wavelength absorption reduces and on red part of visible spectrum i.e. 600-800nm, effect of light trapping is more pronounced to compensate for the less absorption. Light trapping due to light scattering and localized surface plasmon resonance interactions by the

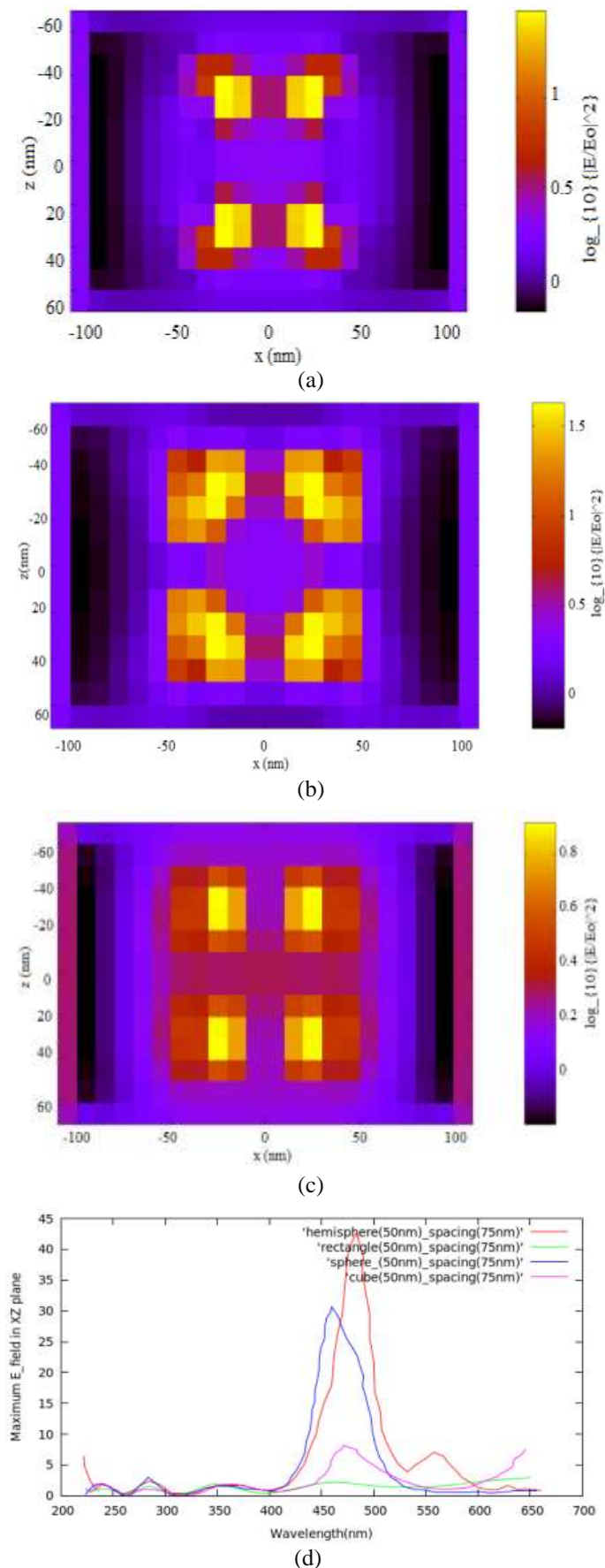


Fig. 2. Snapshot of Electric field near Ag NPs with shapes (a) spherical, (b) hemispherical, (c) cubical and (d) E field variations at the front surface for different shapes

nanoparticles will result in the enhancement of both the optical and electrical properties due to the reduction in the recombination rates in the photoactive layer [14]. Ag demonstrates lower parasitic light absorption, when placed at the front interface reduces the initial reflection and well-tuned Ag NPs can produce the best performance enhancement with plasmonic resonance frequency in the visible and near infrared spectral range.

When LSPR is excited, scattering and absorption occurs simultaneously and only energy scattered by MNPs is useful while absorption in MNPs undermines solar cell performance due to loss of incident light and thermal effect [15]. Numerical calculation and near-electric field distribution of Ag NPs of different sizes and shapes were simulated for a-Si:H photovoltaic devices to obtain strong resonance and higher scattering cross-section. In the first part of our analysis, scattering from Ag nanoparticles are treated analytically to investigate the dependence of shape and surrounding medium. In the second part, scattering from nanoparticles of different diameters/dimensions with constant spacing between them and in third part spacing variations with constant diameters are simulated. Surface coverage analysis with nanoparticle count variations at constant diameter and particle separations are simulated as fourth and final part. This systematic study is to explore several combinations of geometrical parameters to identify the combinations that plays significant role in scattering and absorption enhancement within the device.

3.1. MNP Shape Variants

In this case, Ag NPs of spherical, cubical, rectangular and hemispherical shapes are considered for analysis. Structures constituting of four Ag NPs of 50nm diameter/dimensions with the spacing of 75nm between them are simulated to understand the effect of shapes on scattering within the device and localized field enhancement. The localized electric field distributions provide an overview of the range of light absorbed into the structure as shown in Fig.2 for different shapes, cubical MNPs have wide spread electric field distribution compared to spherical MNPs denoting higher device absorption. Below 400nm a-Si:H absorbs all the incident light and Ag having plasmon resonance within 400-500nm range scatters maximum incident light and a sharp jump in the electric field is observed as shown in Fig. 2(d). In case of a hemisphere compared to a sphere, the reduced spacing between the MNPs and the high-index a-Si:H medium leads to increase in the fraction of light that is scattered into it while compromising on the scattering cross-section of the particles [16] with higher generated fields.

The absorption and scattering efficiencies calculated using Mie scattering principle across visible range of wavelength are as shown in below Fig.3. The cubical nanoparticles with higher exposure to the incident radiations compared to spherical/rectangle structures results in relatively strong scattering and low absorption simultaneously, so that most of the energy in LSPR is scattered by Ag NPs. The undesirable light absorption by the Ag nanoparticles will reduce the number of radiations

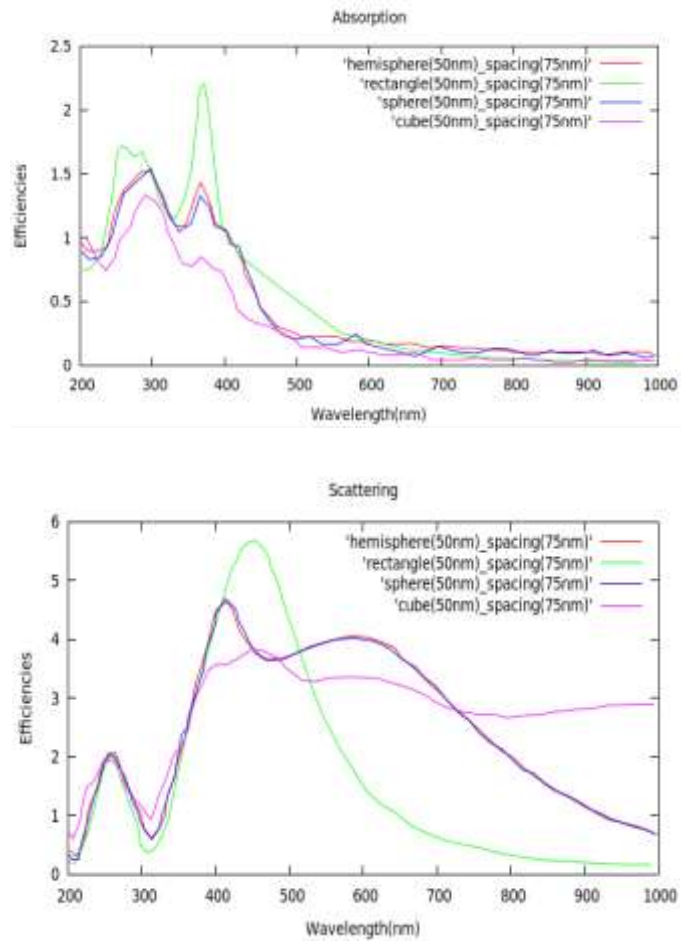


Fig. 3. Absorption and scattering efficiency with varying function of incident wavelength

entering the optical layers, hence reduction in light absorption in layers of a-Si:H structures. On the blue side of the spectrum, from 350-500 nm scattering due to MNP is increasing with absorption almost constant resulting in higher scattering contribution over absorption on extinction cross section. On the red side of the spectrum above 700nm, cubical nanoparticles outperform others in enhanced scattering and reduced absorption. Cubical Ag NPs with higher scattering and reduced absorption compared to other shapes with better electric field distribution at resonance is an ideal choice for plasmonics in thin film a-Si:H cells. The general trend is that the resonance peak is red-shifted with NPs of shapes having a higher overlapping area with the substrate. The most efficient absorption enhancement is observed in structures with rectangular Ag NPs when compared with spherical and cubical Ag NPs with comparatively lower field generation at resonance.

3.2. MNP Size Variants

In this section, spherical and cubical Ag NPs sizes are varied with a constant spacing of 50nm between them to understand the effect of sizes on NP scattering and absorption with electric field distribution on the front surface of a-Si:H solar cells. MNPs size would be of particular interest for light trapping because they have a direct

influence on the extinction efficiency in the wavelength range where light trapping is highly needed for a-Si:H. Near-field plots of structures with different MNP sizes as shown in Fig.4 establish the relation between transmission of the electric field within the nanoparticle and the a-Si:H substrate at the resonant wavelength providing correlation for optical and electrical enhancement. With the increase in NP size, the movement of conduction band electrons will weaken the NP center field of polarization resulting in the reduction of force from NPs on electronics and red-shift of plasmon resonance peak. The surface plasmon resonance peak attenuation for higher sizes will reduce NP absorption and enhance device scattering [17].

The size of the particles should be optimized for the desired application to get strong extinction (scattering and absorption) [18]. For samples with particle counts of four and diameters of 25, 50, 75 and 100nm, the absorbed and scattered fractions were measured. As the NP sizes are increased, red shift with the broadening of the plasmon resonance is observed resulting in positive scattering enhancing broad band light trapping across visible range spectrum. It is observed that small size NPs efficiently couple the incident light into a-Si:H due to near field effect generated by the surface plasmon excitation of Ag NP. The results demonstrate that with increasing particle size the absorbed fraction in device increases. However, the results shown in Fig.5 indicate that extinction is dominated by NP absorption for 25nm particles and with an increase in the size of the particles, extinction is dominated by scattering.

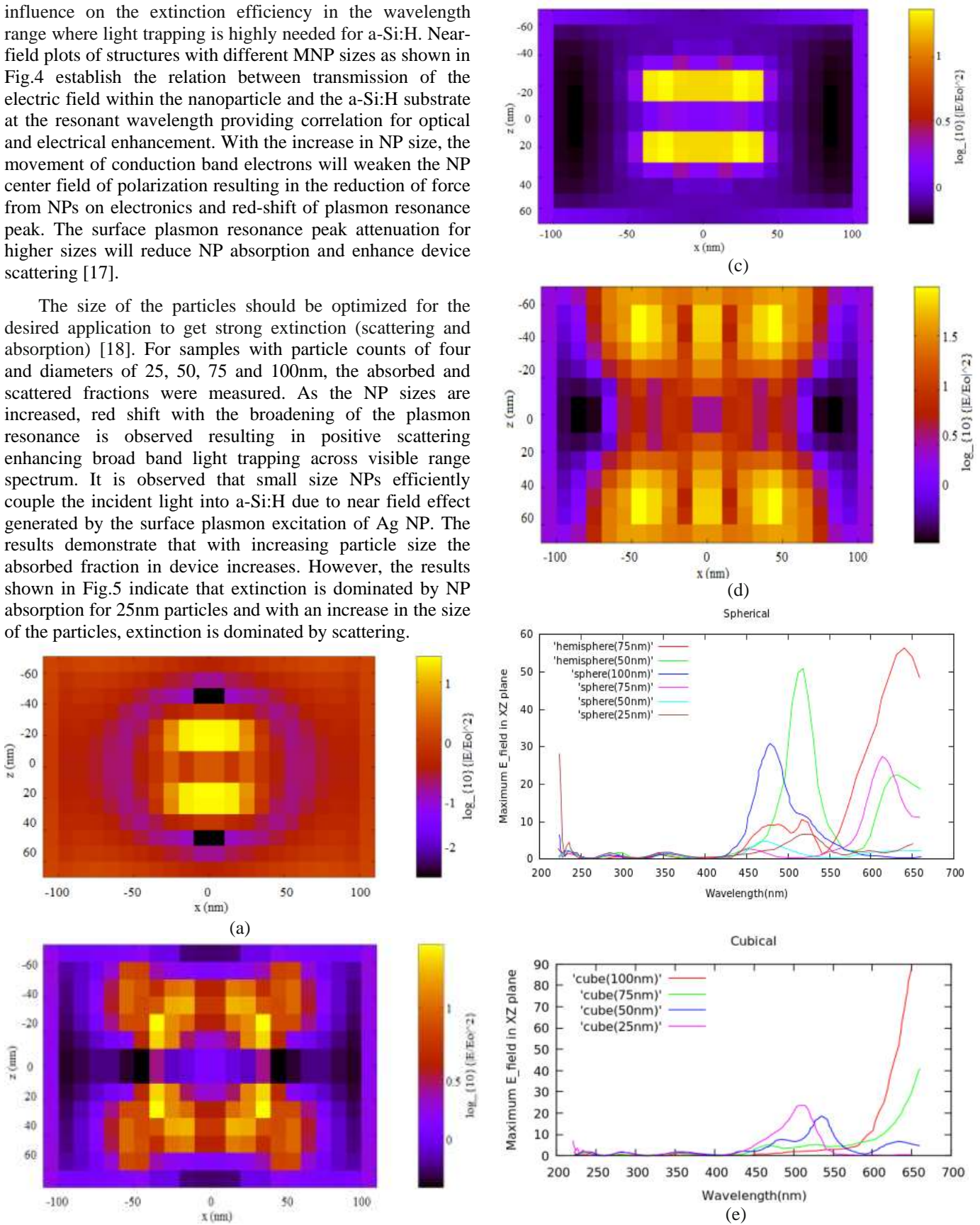


Fig. 4. Snapshot of Electric field near Ag NPs (a) spherical (25nm), (b) spherical (100nm), (c) cubical (25nm), (d) cubical (100nm), (e) E field variations at the front surface for spherical and cubical NPs for different sizes

The increased NP absorption of small size NPs will lead to loss of incident light and negative thermal effects. As the size of NPs increases, conduction electrons across the particle no longer move in phase, the polarizability of metallic NPs will be lower and will further lead to multilevel resonance mode resulting in more energy being scattered into the active layer of thin film solar cell.

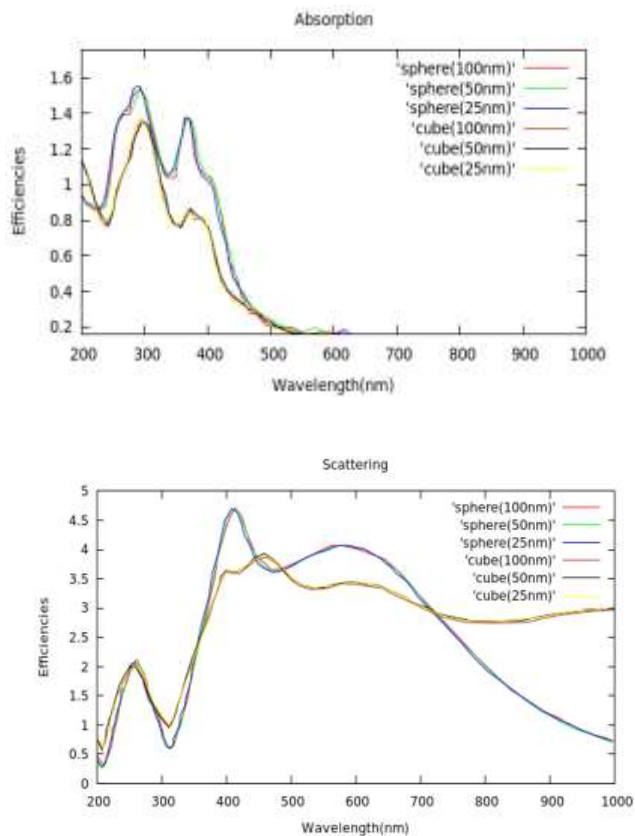


Fig. 5. Absorption and scattering efficiency with varying function of incident wavelength

Considering the ease of nanoscale fabrication, large structures are preferred over small structures but too large the size will lead to multiple oscillations resulting in the reduction of scattering efficiency. Additionally, the relative contribution of absorption to extinction decreases with size, resulting in predominantly scattering nanoparticles for diameters above 50nm. For small particles supporting only dipolar modes, the total extinction cross section consists of a large absorption cross section and a smaller scattering cross section. For larger particles, with diameters of 100 nm or larger, the opposite is true: although the total extinction cross section remains dominated by dipolar contributions, the scattering cross section is much larger than the absorption cross section. Due to excitation of plasmonic resonances, strongest parasitic absorption is observed with the strongest scattering for light-trapping which may cause hindrance for positive scattering and limit the cell performance, for larger NPs balance between scattering and parasitic absorption will be crucial for higher performance.

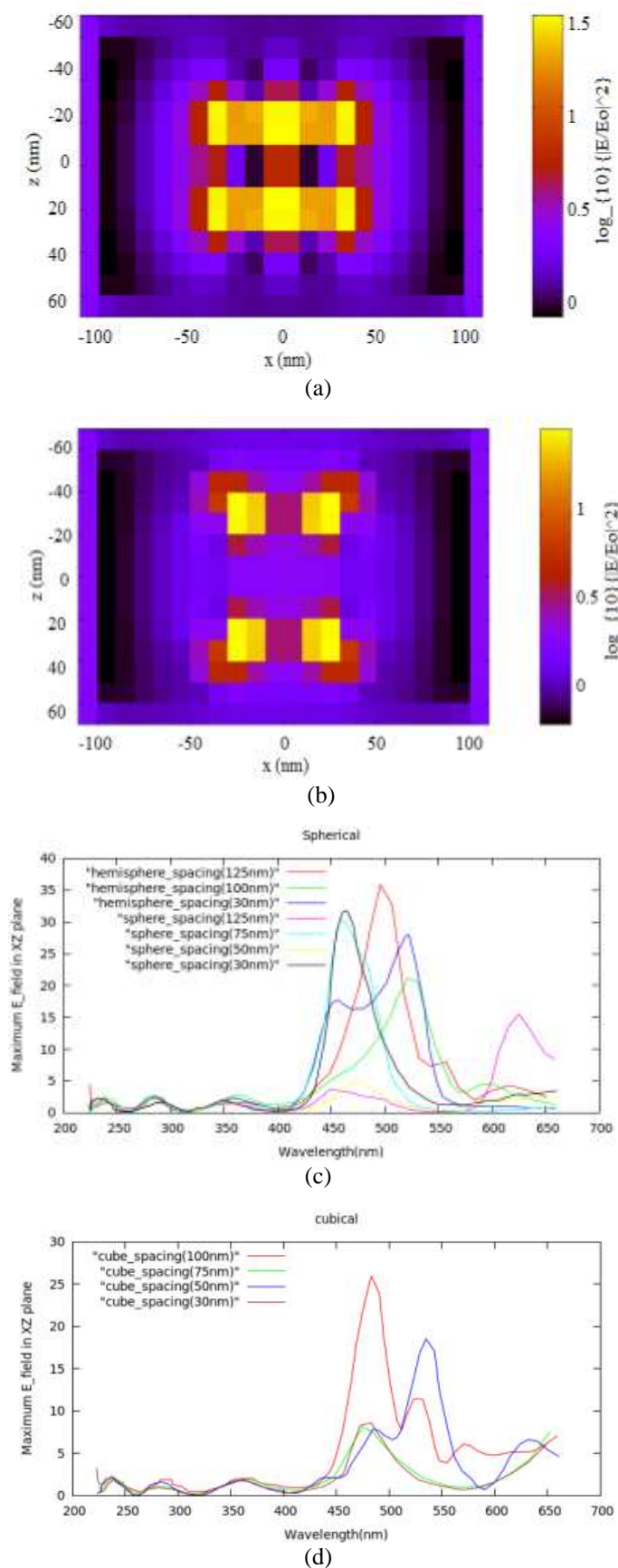


Fig. 6. Snapshot of Electric field near Ag NPs (a) spherical with spacing of 30nm, (b) spherical with spacing of 75nm, (c) & (d) E field variations at the front surface for spherical and cubical NPs for different spacing's.

3.3. MNP Spacing Variants

In this section, structures with four Ag NPs of 50nm diameter with different spacing between them are simulated to understand the role of periodicity on scattering and light absorption in the devices. From Fig.6, the influences on LSPR of metallic NPs by its periods can be well summarized as: (1) For lower periods(near to 50nm), as metallic NPs are setting close, the peak of resonance will move to shortwave direction, the intensity of resonance will also be strengthened which lead to a stronger scattering and will have a contribution to light absorption in solar cell, however, excessively close an array(around 30nm) may greatly block incident light, and it leads to no transmission in metallic NPs and prevents light from reaching the active layer when introduced into solar cell. (2) For higher periods (around 200nm), too wide an array undermines the interaction between metallic NPs, resembling resonance similar to one excited by a single metallic NP, and the effect of electric resonance disappears. Moreover, for widely spaced particles, the effect of nanoparticles can be almost disregarded and the structure converges to the case with no nanoparticles. The comparatively larger separation between nanoparticles at the top allow more incident light to penetrate into conducting substrate, the results in Fig.6 and Fig.7 show that surface plasmon excitation of small radius NPs with large separation greatly enhances the light transmittance in the visible wavelength region dominated by the scattering and the near-field enhancement.

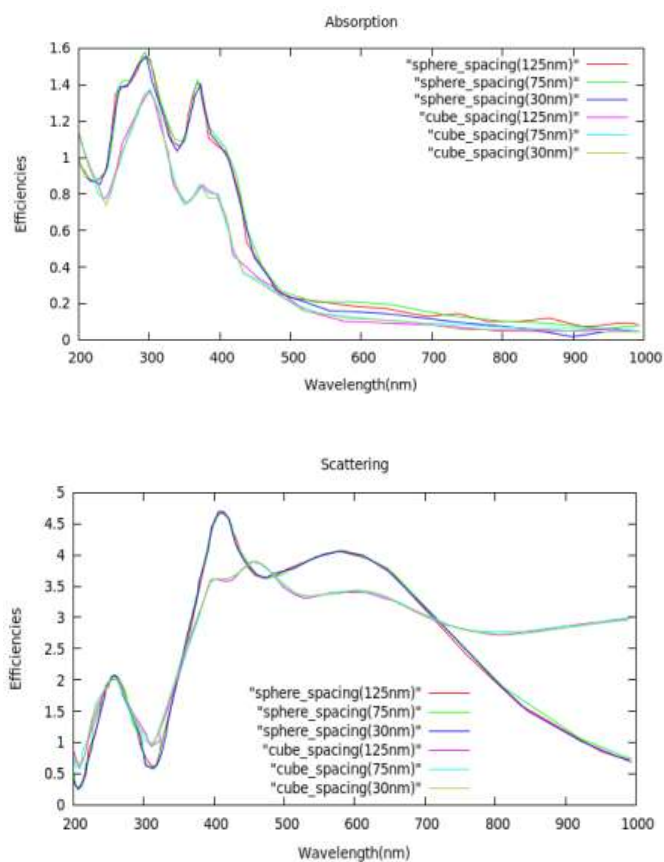


Fig. 7. Absorption and scattering efficiency with varying function of incident wavelength

Fig.7 shows that position of the peak shifts to blue with increase in value when the period increases from 75nm to 125nm, meanwhile more obvious absorption peaks appear in the near infrared range leading to more light absorption. With the increase in spacing, the SPP red shifts and higher modes appear, resulting in multiple absorption enhancement bands at longer wavelengths. The coupling between NPs due to spacing is an important consideration for plasmonic light trapping. The NPs when closely spaced (30nm), the generated surface oscillations will be in opposite directions for adjacent NPs at resonance leading to radiating waves getting cancelled out resulting in heat dissipation and lower radiation efficiency. So for closely spaced particles, broadening of plasmon resonance with the large nonradiative loss due to strong coupling is observed. Increasing the spacing causes a decoupling of MNPs and in turn weakens the nonradiative loss. Therefore, increase in spacing results in light transmission enhancement and upon a further increase in the spacing, a decrease in the transmission is seen.

3.4. MNP Coverage Variants

In this section, structures with different counts of 50nm dimension NPs having a spacing of 50nm between them are simulated. The structure front surface area of 400 x 250 nm² and with altering count of Ag NPs, analysis to understand the significance of surface coverage on the generation of localized electric field and scattering/absorption is covered. For balanced NP spread across X-Z plane and to maintain symmetry, structures with an even count of 4, 6 and 8 NPs are simulated, obtained localized electric field are as shown in Fig.8 and the extinction efficiencies as shown in Fig.9.

Structures with 8 NPs having a surface coverage of around 63% exhibits localized electric field dominated by near field coupling as shown in Fig 8(a) and 8(c) with no longer NPs behave as isolated particles. In the considered scenario, with 4 NPs, surface coverage will be around 32% and isolated particles will have higher electric field values compared to 63% coverage as shown in Fig 8(b) and 8(d). Similarly, with 6 NPs, the surface coverage would be around 48% resulting in NP absorption higher than 4 NP and less than 8 NP structures. The simulated results show that cubical NPs outperform spherical NPs in electric field distributions across multiple surface coverages. Lower the surface coverage, NPs scattering is also less and with higher surface coverage, scattering within the devices and an undesired NP absorption is rising as shown in Fig.9. LSPR modes for Ag NPs fall in the visible spectral region [19] and can be systemically tuned from 400nm to 800nm by size, shape and distribution variations of MNPs where a-Si:H solar cells require efficient light trapping as illustrated in above sample of structures. On the whole, NP related parameters will concentrate all the incident radiations into device parallelly blocking the radiations to go out of the device covering wide wavelength range. The obtained results from all the considered test cases show that the NPs with shapes of higher substrate overlapping area and larger sizes, placed at average spacing covering half the exposed area result in red-shift of resonance, improving the absorption power across

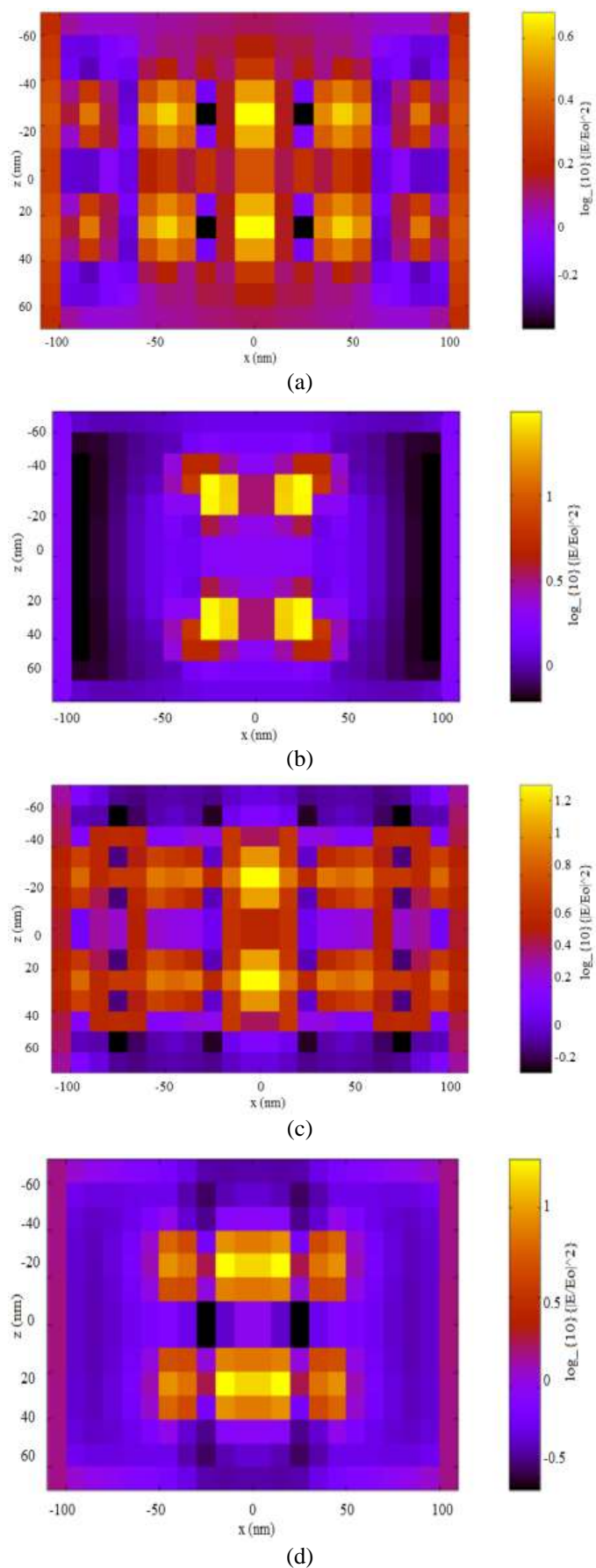


Fig. 8. Snapshot of Electric field near Ag NPs (a) Eight spherical, (b) Four spherical, (c) Eight cubical, (d) Four cubical

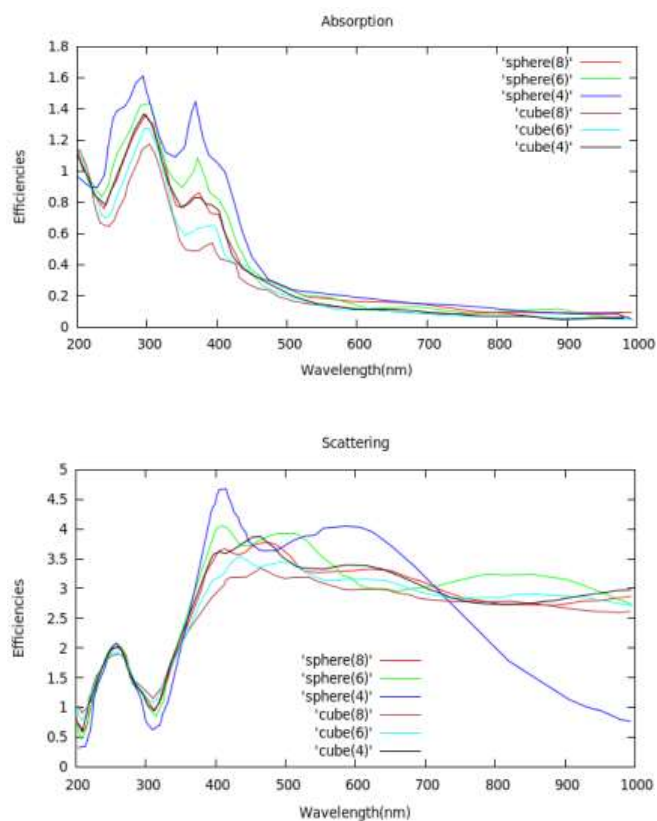


Fig. 9. Absorption and scattering efficiency with varying function of incident wavelength

the visible range of spectrum upon exposed to light radiations.

4. Conclusion

The comparative and analytical analysis of structures with Ag NPs at the front surface of a-Si:H is performed covering NPs as a function of size, shape, periodicity and surface coverage for higher device performance. The summary of obtained results with variations are as follows: the resonance shift is seen with cubical NPs over spherical NPs from 454nm to 480nm with an enhanced electric field resulting in 200% increase in device scattering near infrared region. The resonance shift from 445nm to 615nm is observed upon increasing the size of Ag NPs from 25 to 75nm with the 10 fold increase in scattering over the NP absorption. The coverage of around 50% and with constant periodicity for balanced spread of NPs exhibits an electric field enhancement of around 150% at around 600nm upon compared to other spacing and NP coverage variants resulting in 20 times higher scattering within the device across the visible range of spectrum. The obtained results presented in the paper enables to narrow down the plasmonic parameters for highly efficient thin film solar cells and the structures with NP patterns where scattering dominates absorption are segregated and will be tested for experimental applications.

References

- [1] Maria Markatou, "Renewable Energy Technologies in Greece: A Patent Based Approach", *International Journal of Renewable Energy Research*, Vol.2, No.4, pp 718-722, 2012
- [2] Zakaria Bouzid, Nassera Ghellai, Tinhinene Mezghiche, "Overview of Solar Potential, State of the Art and Future of Photovoltaic Installations in Algeria", *International Journal of Renewable Energy Research*, Vol.5, No.2, pp 427-434, 2015
- [3] Jialin Liu, Raymond Hou, "Solar Cell Simulation Model for Photovoltaic Power Generation System", *International Journal of Renewable Energy Research*, Vol.4, No.1, pp 49-53, 2014
- [4] Velamuri Suresh, Sreejith S, "Economic Dispatch and Cost Analysis on a Power System Network Interconnected With Solar Farm" *International Journal of Renewable Energy Research*, Vol.5, No.4, pp 1098-1105, 2015
- [5] K R Catchpole, A Polman, "Design Principles for Particle Plasmon enhanced solar cells", *Appl. Phys. Lett.* 93, 191113, 2008, doi:10.1063/1.3021072
- [6] S A Maier, "Plasmonics: Fundamentals and Applications", Springer, New York, 2007, doi: 10.1007/0-387-37825-1
- [7] U Dasgupta, S K Saha, A J Pal, "Plasmonic effect in pn-junction solar cells based on layers of semiconductor nanocrystals: Where to introduce metal nanoparticles?", *Solar Energy Materials and Solar Cells*, Vol 136, pp 106-112, 2015
- [8] H Y Choi, M S Guerrero, M Aquino, C Kwon, Y S Shon, "Preparation of Gold Nanoisland Arrays from Layer-by-Layer Assembled Nanoparticle Multilayer Films", *Bull. Korean Chem. Soc*, Vol. 31, No. 2, pp 291-297, 2010.
- [9] A F Oskooi, D Roundy, M Ibanescu, P Bermel, J D Joannopoulos, S G Johnson, "MEEP: A flexible free-software package for electromagnetic simulations by the FDTD method", *Computer Physics Communications*, Vol 181, No 3, pp 687-702, 2010
- [10] Edward Palik, "Handbook of optical constants of solids", Academic Press, Elsevier Science, pp 350-356, 1985
- [11] A Vora, J Gwamuri, J M Pearce, P L Bergstrom, D O Guney, "Multi-resonant silver nano-disk patterned thin film hydrogenated amorphous silicon solar cells for Staebler-Wronski effect compensation", *AIP Journal of Applied Physics*, Vol 116, No 9, 2014
- [12] P R West, S Ishii, G V Naik, N K Emani, V M Shalaev, A Boltasseva, "Searching for better plasmonic materials", *Laser and Photonics Reviews*, Vol 4, No 6, pp 795-808, 2010
- [13] K L Kelly, E Coronado, L L Zhao, G C Schatz, "The Optical Properties of Metal Nanoparticles: The Influence of Size, Shape, and Dielectric Environment", *Journal of Physical Chemistry B*, Vol 107, No 3, pp 668-677, 2003
- [14] M J Mendes, S Morawiec, T Mateus, A Lyubchyk, H Aguas, I Ferreira, E Fortunato, R Martins, F Priolo, and I Crupi, "Broadband light trapping in thin film solar cells with self-organized plasmonic nano-colloids", *Nanotechnology*, Vol 26, No 13, 2015
- [15] D Duche, P Torchio, L Escoubas, F Monestier, J J Simon, F Flory, G Mathian, "Improving light absorption in organic solar cells by plasmonic contribution", *Solar Energy Materials and Solar Cells*, Vol 93, No 8, pp 1377-1382, 2009
- [16] Z Ouyang, X Zhao, S Varlamov, Y Tao, J Wong, S Pillai, "Nanoparticle-enhanced light trapping in thin-film silicon solar cells", *Progress in Photovoltaics*, Vol 19, No 8, pp 917-926, 2011
- [17] N C Lindquist, P Nagpal, K M McPeak, D J Norris, Oh S-H, "Engineering metallic nanostructures for plasmonics and nanophotonics," *Reports on Progress in Physics Physical Society*, Vol 75, No 3, 2012
- [18] E Ringe, M R Langille, K Sohn, J Zhang, J Huang, C A Mirkin, R P Van Duyne, L D Marks, "Plasmon Length: A Universal Parameter to Describe Size Effects in Gold Nanoparticles", *The Journal of Physical Chemistry Letters*, Vol 3, No 11, pp 1479-1483, 2012
- [19] X H Liu, L X Hou, J F Wang, B Liu, Z Sen Yu, L Q Ma, S P Yang, G S Fu, "Plasmonic-enhanced polymer solar cells with high efficiency by addition of silver nanoparticles of different sizes in different layers", *Solar Energy*, Vol 110, pp 627-635, 2014